Inelastic scattering of ^{16}O by even mass nickel isotopes*

Leon West, Jr.† and N. R. Fletcher
Department of Physics, The Florida State University, Tallahassee, Florida 32306
(Received 18 October 1976)

The angular distributions of ^{16}O inelastically scattered from enriched targets of even mass nickel isotopes measured over the angular range $\theta_{c.m.} \sim 50°$ to 170° are presented. The measured cross sections are compared with the results of distorted-wave Born approximation calculations for inelastic scattering which employ the conventional four parameter optical potential or a folded excitation potential. The folded method improves the description of the data in some cases but does not provide a consistent improvement for all energies and isotopes.

[NUCLEAR REACTIONS $^{58,60,62,64}Ni(^{16}O, ^{16}O')Ni^*(2^+)$, measured $\sigma(\theta)$ at $E_{lab}=42$ and 48 MeV. Calculated $\sigma(\theta)$ by DWBA using conventional and folded potentials. Deduced deformation lengths.]

I. INTRODUCTION

Although heavy ion scattering and reactions have been studied for some time, it is only relatively recent that the interference effect between the Coulomb and nuclear contribution to the inelastic scattering process has been reported.[1] Shortly after the initial report, the interference was described through the use of distorted-wave Born approximation (DWBA) codes which had been extended to incorporate contributions from high angular momenta and very large radii.[2-4] It was shown in one example[2] that the results of a DWBA calculation did not provide a good description of the $^{58}Ni(^{16}O, ^{16}O')^{58}Ni^*(2^+)$ inelastic scattering even when the Coulomb and nuclear deformations were allowed to have different values. In an attempt to correct this situation a folded potential approach to heavy ion inelastic scattering was developed.[5] More recent calculations for inelastic heavy ion scattering have included coupled channels and nuclear reorientation effects[6,7] in an effort to explain the inadequacies of the collective model DWBA[8] approach when applied to heavy ion inelastic scattering.

The present work reports on measurements of the inelastic scattering of ^{16}O ions from the even mass stable Ni isotopes, leaving the target nucleus in the first excited ($J^\pi = 2^+$) state. In addition a comparison is made between the collective model DWBA approach to explaining the results and that using a folded potential.[5] The deformation lengths obtained for different isotopes and bombarding energies are found to lie within the limits set by other inelastic scattering results. The experimental procedures have been reported in an earlier publication of the elastic scattering results.[9]

II. DWBA FORMALISM FOR INELASTIC SCATTERING

The DWBA formalism for inelastic scattering as used in this work has been outlined in an earlier report.[2] The transition amplitude is largely determined by a sum over values of orbital angular momenta of the radial integrals which have the form,

$$I_{l_f l_i} = \int_{r=0}^{\infty} U_{l_f}(r)\overline{V}_l(r)U_{l_i}(r)dr\,.$$

The inelastic scattering interaction potential $\overline{V}_l$ consists of Coulomb and nuclear parts as

$$\overline{V}_l(r) = \overline{V}^C_l(r) + \overline{V}^N_l(r)\,,$$

and for single excitation to the low lying $J^\pi = 2^+$ state the value of l is limited to 2.

In the collective model DWBA[8] these potentials for target excitation are written as

$$\overline{V}^N_{l=2}(r) = -\beta_2^N \frac{R_T}{a}(U + iW)\frac{e^x}{(1+e^x)^2}\,,$$

where

$$x = \frac{r-R}{a}$$

and

$$\overline{V}^C_{l=2}(r) = \frac{3}{2l+1}\beta_2^C R_{CT}{}^2 Z_T Z_P e^2 \begin{cases} r^2/R_C{}^5\,, & r<R_C \\ 1/r^3\,, & r\geq R_C \end{cases}$$

The nuclear deformation parameter β_2^N describes the magnitude of the quadrupole deformation of the nuclear potential (in both vibrational and rotational models) resulting from the nuclear interaction between the projectile and the target. The Coulomb

deformation parameter β_2^C describes the corresponding quantity in the Coulomb interaction of the two nuclei. For the model of a uniform charge distribution of sharp radius R_{CT}, the value of β_2^C is related to the reduced transition probability value by the expression

$$B(E2\uparrow)=\left(\frac{3}{4\pi}eZ_T\beta_2^C R_{CT}{}^2\right)^2 .$$

The above form for $\overline{V}_l^N$ is a four parameter potential. Although six parameter studies of ^{16}O + Ni have been done, an extensive investigation[9] of the elastic scattering potential parameters has indicated that in actual fact as few as two parameters are sufficient to describe the ^{16}O + Ni potential — the Igo parameters C_U and C_W.[9-11] It is therefore felt that the parametrization here in terms of the real and imaginary well depths U and W (with the radius parameter r_0 and the diffuseness a having assigned values) should be adequate. The radius of the nuclear potential is parametrized in this study as

$$R=r_0(A_P{}^{1/3}+A_T{}^{1/3})=r_0A_P{}^{1/3}+R_T$$

with the radius parameter fixed at $r_0=1.22$ fm throughout this work. The Coulomb radius of the target, R_{CT}, is assumed equal to the nuclear radius of the target, i.e., $R_{CT}=R_T$, and the total Coulomb radius is assumed to be $R_C=R$. The nuclear potential diffuseness is assigned the value $a=0.50$ fm.

In an alternative approach for description of the inelastic scattering, a folded potential was developed[5] in an effort to account for effects of the finite size of the projectile. The folding procedure used provides a consistent treatment of both elastic and inelastic scattering. Starting from the single-fold nucleon plus nucleus potential of Eq. (3), Ref. 9,

$$V(\vec{r})=\int_T V_{NP}(\vec{r}-\vec{r}_T)\,\rho_T(\vec{r}_T)\,d\vec{r}_T ,$$

we use the deformed density prescription[12] to form the transition density given by

$$\rho_T(r_T,\theta)=\rho_T^0\beta_2^N\frac{R_T}{a_T}F_2(r_T)\frac{1}{\sqrt{2\pi}}P(\cos\theta) .$$

The derivative form factor $F_2(r_T)$ is given for a Woods-Saxon matter distribution as

$$F_2(r_T)=\exp\left(\frac{r_T-R_T}{a_T}\right)\left[1+\exp\left(\frac{r_T-R_T}{a_T}\right)\right]^{-2} .$$

The parameters R_T and a_T are estimated by assuming the matter distribution is identical to the charge distribution and then using radius and diffuseness parameters as determined by electron scattering.[13] The constant ρ_T^0, is determined by the target geometric parameters and mass number as in Ref. 9. The single folded integral is then evaluated by making a numerical Legendre expansion of a Woods-Saxon form of V_{NP} written as

$$V_{NP}(r')=-(U_{NP}+iW_{NP})\left[1+\exp\left(\frac{r'-R_{NP}}{a_{NP}}\right)\right]^{-1} ,$$

where U_{NP} is the effective real well depth of the nucleon plus projectile nuclear potential interaction. The imaginary well depth remained that derived from the Woods-Saxon form. For the inelastic folded calculation, the folded Coulomb potential contribution to $\overline{V}_l$ was used rather than the conventional form.

Assuming that the potential parameters can be reasonably well determined from parametrization of the elastic scattering cross section and that β_2^C is determined by the $B(E2)$ value, then one might be able to determine if the nuclear quadrupole deformation length $\delta^N=\beta_2^N R_T$ differs significantly from the corresponding electromagnetic quantity. Section IV contains a comparison of the extracted nuclear deformation lengths to the Coulomb deformation lengths for the targets ^{58}Ni, ^{60}Ni, ^{62}Ni, and ^{64}Ni.

DWBA calculations were performed on the Florida State University CDC 6600 computer with the computer code KULNUC, a hybrid DWBA program based upon Kunz's code DWUCK [14] and Samuel and Smilansky's code ITER.[15] The code KULNUC was written to calculate the differential cross section for heavy ion inelastic excitation of the target nucleus ($J^\pi=0^+\rightarrow 2^+$) where large values of angular momentum and interaction radius are involved. The Samuel and Smilansky technique[15] circumvents the integration problem by making use of the fact that for large partial wave numbers l_f the nuclear contributions to the inelastic scattering interaction potential and the radial wave function, and hence to the integral I_{l_f,l_i}, become insignificant. The code KULNUC was compared to both the DWBA code DWUCK and the classical Coulomb excitation code COULEX [16] in the limits where these programs are valid.

III. ANALYSIS OF DATA

Angular distributions for ^{58}Ni(^{16}O, ^{16}O)-^{58}Ni*(2^+, 1.45 MeV) are illustrated in Fig. 1 at the laboratory energies of 36, 42, and 48 MeV. The solid line of Fig. 1(a) is the cross section calculated with the conventional potential approach using potential parameters which describe the elastic scattering differential cross section at 36 MeV. The calculated cross section is within 2% of that for pure Coulomb excitation, as is expected since the well depths were extracted[9] from an elastic scattering cross section that is almost a Ru-

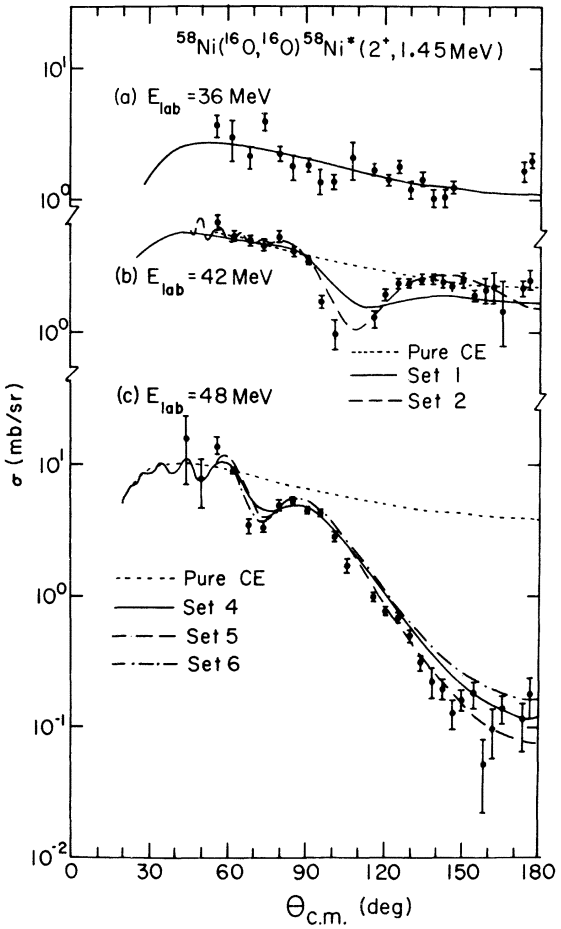

FIG. 1. Measured and calculated cross sections for ^{58}Ni(^{16}O, ^{16}O)^{58}Ni*(2$^+$). The cross sections were calculated using the potential parameter sets of Table I.

therford cross section. The magnitude is reproduced by use of the known quadrupole electromagnetic transition probability value $B(E2) = 0.0726\, e^2 b^2$.[17] Videbaek *et al.*[1] reported a smaller value of $B(E2) = 0.066\, e^2 b^2$ which was extracted from analysis of $^{16}O + ^{58}Ni$ inelastic scattering at similar energies. The experimental data here are not adequate to distinguish between the two values.

Figure 1(b) indicates that the angular distribution for ^{58}Ni(^{16}O, ^{16}O)^{58}Ni* at a bombarding energy of 42 MeV is reproduced qualitatively with the optical model potential parameters, Set 1 of Table I, which fit the elastic scattering angular distribution. Results of another calculation based on optical parameters (Set 2, Table I), which provide a better description of the 42 MeV elastic scattering data in the neighborhood of grazing where the Coulomb nuclear interference is strongest, are also shown in Fig. 1(b). The parameter set 2 has a very small absorptive term and its use results in a more prominent minimum in the calculated inelastic scattering and, consequently, better agreement with the data. Also for this calculation $\beta_2^N = 1.2\,\beta_2^C$. The optical parameters of Set 2 were obtained by performing a least squares minimization having truncated the elastic data at $\theta_{c.m.} = 125°$. The procedure produces a small absorption ($W/U \sim 0.03$) similar to an earlier investigation at 44 MeV.[3]

The angular distribution for ^{58}Ni(^{16}O, ^{16}O)^{58}Ni* at a laboratory energy of 48 MeV is shown in Fig. 1(c). The potential parameters of Set 4, which describe the complete elastic scattering angular distribution, produce good agreement with the data. Again, the use of a small imaginary well depth (Set 5) produces better agreement. Parameter set 5 was generated by fixing the value of the imaginary well depth at 10 MeV and then searching for the real well depth which best reproduced the elastic scattering data in the angular range $\theta_{c.m.} \leq 125°$. In the elastic channel, data forward of 125° are reproduced better with Set 5, especially near the grazing maximum, but the predicted cross section at 176° is an order of magnitude lower than the experimental cross section. For these inelastic calculations at 48 MeV we hold $\beta_2^N \equiv \beta_2^C$. Increasing the parameter β_2^N relative to β_2^C merely multiplies the

TABLE I. Optical model parameter sets used in inelastic scattering calculations. Unless otherwise noted the real and imaginary well depths, U and W, were varied to provide the best description of the entire measured elastic angular distributions (Ref. 9) with $r_0 = 1.22$ fm and $a = 0.50$ fm in a four parameter optical model.

Set	Nuclides	E_{lab}	U	W
1	$^{16}O + ^{58}Ni$	42	87.5	21.1
2[a]		42	96.6	3.0
3[b]		42	19.6	21.1
4		48	93.1	34.4
5[a]		48	92.8	10.0
6[b]		48	19.5	34.4
7	$^{16}O + ^{60}Ni$	42	96.6	30.5
8[a]		42	100.0	13.9
9		48	107.7	38.4
10	$^{16}O + ^{62}Ni$	42	100.1	37.2
11[a]		42	107.0	24.2
12		48	102.6	19.5
13	$^{16}O + ^{64}Ni$	42	114.5	49.8
14[a]		42	131.2	24.4
15		48	129.4	51.5

[a] Optical parameters obtained by describing the elastic data limited to $\theta_{c.m.} \leq 125°$.

[b] Folded potential calculations where only the real nucleon plus projectile potential is varied while the imaginary potential remains at the value determined in a conventional treatment of elastic scattering. Geometry parameters are $r_{NP} = 1.24$ fm, $a_{NP} = 0.64$ fm, $r_T = 1.06$ fm, and $a_T = 0.57$ fm.

calculated cross section by an approximate amount $(\beta_2^N/\beta_2^C)^2$ over the back angles, resulting in even poorer agreement with the data in this angular range. Slight improvement of the fit does occur in the angular region of the interference minimum when a larger value of β_2^N/β_2^C is used.

Because of the obvious difficulties in parametrizing the measured inelastic cross section of 42 and 48 MeV, the folded potential approach was tried. The folded potential parameters which describe the 42 MeV elastic scattering data, Set 3, Table I, are used to produce the dashed and solid curves of Fig. 2. The use of $\beta_2^N = 1.3\beta_2^C$ greatly improves the fit. For comparison, the dot-dash curve of Fig. 2 corresponds to the conventional set 1, with $\beta_2^N = 1.3\beta_2^C$. At 48 MeV the best results are obtained from folded potential set 6 and when $\beta_2^N = \beta_2^C$, it produces the dot-dash curve of Fig. 1(c). The calculated cross sections near the interference minimum more closely reproduce the data than do the conventional calculations; however, it is still necessary to allow the ratio β_2^N/β_2^C to vary.

The inelastic scattering from ^{60}Ni at 42 and 48 MeV is shown in Fig. 3. The larger known $B(E2)$ value[18] of 0.097 e^2b^2 for ^{60}Ni is evident at forward angles where the dominant Coulomb excitation produces larger cross sections than for ^{58}Ni. The results of calculations based on parameter sets 7 and 9 which best reproduce the elastic scattering data are shown as the solid curves. Both of these sets have large imaginary well depths but reproduce the inelastic data fairly well. The interference minimum is better reproduced again by using optical parameters, Set 8, which fit the elastic scattering data truncated to $\theta_{c.m.} \leq 125°$. The imaginary well depth of Set 8 is approximately one-third that of Sets 7 and 9 and it provides a small improvement in the fit. In all curves of Fig. 3, $\beta_2^N = \beta_2^C$. When the ratio β_2^N/β_2^C is increased, the calculated inelastic cross section has the desired more prominent minimum but it is larger than the measured cross section for $\theta_{c.m.} \gtrsim 130°$.

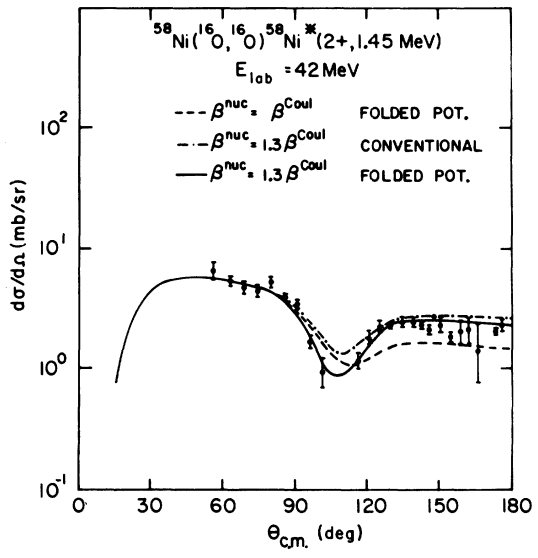

FIG. 2. Cross sections calculated with the folded potentials (Set 3, Table I) are compared with data and a cross section calculated with the conventional potentials (Set 1, Table I). The relative values of the nuclear and Coulomb deformation parameters are indicated.

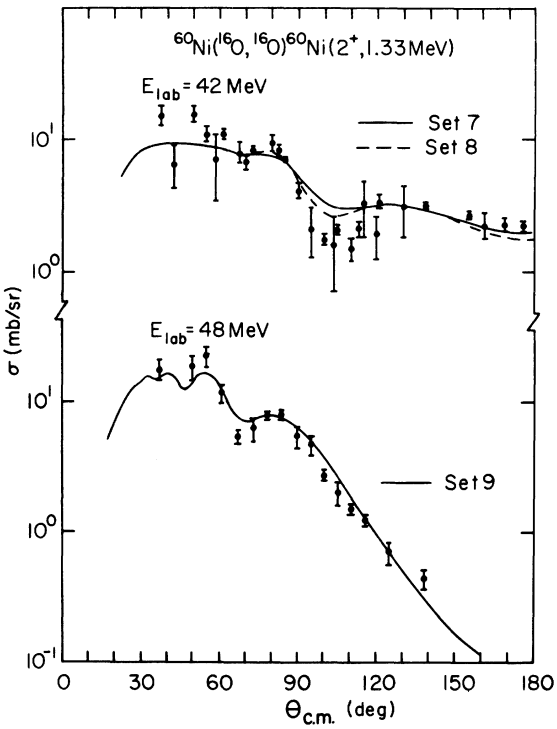

FIG. 3. Measured and calculated cross sections for $^{60}Ni(^{16}O,^{16}O)^{60}Ni^*(2^+)$. The potential parameter sets are those of Table I.

The inelastic scattering data of 42 and 48 MeV from targets of ^{62}Ni and ^{64}Ni are presented in Figs. 4 and 5 along with some curves representing calculated cross sections. The solid curves are results of inelastic scattering calculations based on optical parameter sets which have been used to reproduce elastic scattering over the entire angular range, whereas the dashed curves are based on truncated elastic scattering data which yield a smaller imaginary well depth. The use of parameters with a smaller imaginary well depth produces a modest improvement to the fit at 42 MeV for ^{64}Ni but not for ^{62}Ni. At 48 MeV the measured angular distributions are reproduced very well by calculations based on the parameters which also describe the elastic scattering; however, slight deviations

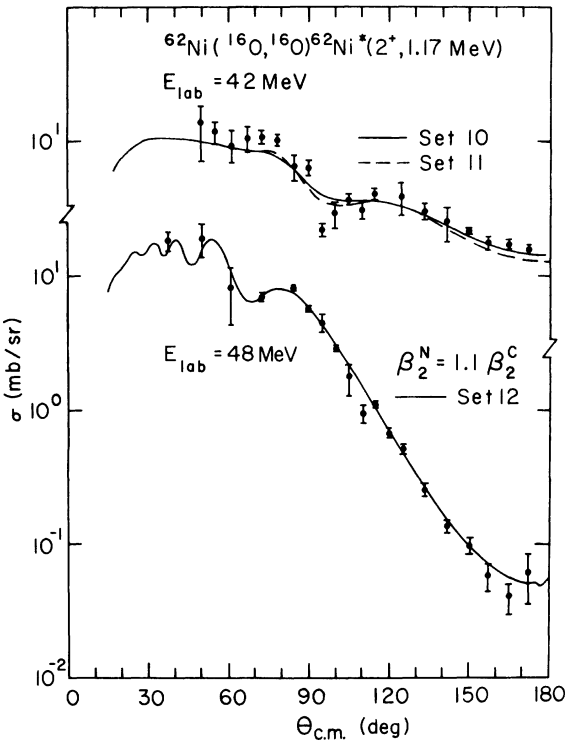

FIG. 4. Measured and calculated cross sections for ^{62}Ni(^{16}O, ^{16}O)^{62}Ni*(2$^+$). The potential parameter sets are those of Table I.

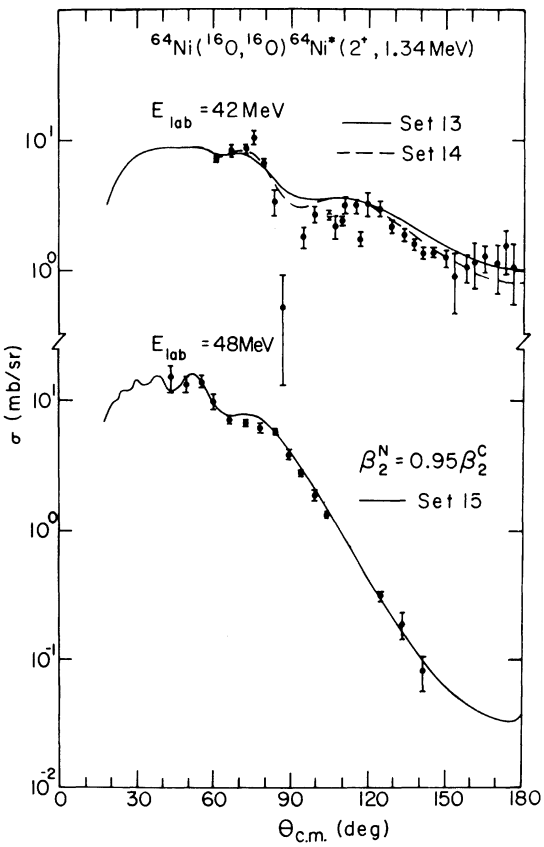

FIG. 5. Measured and calculated cross sections for ^{64}Ni(^{16}O, ^{16}O)^{64}Ni*(2$^+$). The potential parameter sets are those of Table I.

from units in the ratio β_2^N/β_2^C are required. In all cases in Figs. 4 and 5, the use of the folded potential does not appreciably improve the agreement.

IV. DISCUSSION AND CONCLUSIONS

As has been confirmed by this investigation and a number of other studies, the DWBA approach can be used to describe the inelastic scattering of heavy ions. In contrast to the elastic scattering results, the four-parameter optical model potential, which is favored by a DWBA parametrization of the inelastic scattering cross section, has a small imaginary well depth ($W/U \simeq 0.1$–0.2). Larger imaginary well depths in the four-parameter optical model, which are necessary to reproduce the elastic scattering data over the entire angular range, do not reproduce the interference structure in the inelastic scattering cross section. The use of a folded potential as the nuclear inelastic scattering interaction potential resulted in considerable improvement in the prediction of the angular distribution for the inelastic scattering of ^{16}O from ^{58}Ni at a bombarding energy of 42 MeV, but only limited improvement for differential cross sections measured at other bombarding energies or for other Ni isotope targets. The use of a folded Coulomb potential in both the elastic and inelastic channels produced little change in the scattering cross sections. This apparently occurs because the conventional and folded forms are identical for radii greater than 8 fm for the case of ^{16}O + Ni while the interior region is obscured by nuclear absorption effects.

Generalizations drawn from the conventional potential parametrization of the inelastic scattering data are as follows. (1) As the imaginary well depth is increased the interference structure becomes less prominent and the cross section at back angles increases. (2) As the real well depth is increased, the interference structure becomes more prominent and the cross section at back angles decreases. (3) As the nuclear deformation parameter is increased relative to the Coulomb deformation parameter, the interference becomes more prominent and the back angle cross section increases approximately proportional to $(\beta^N/\beta^C)^2$.

The various nuclear deformation lengths which have been extracted from the analysis of the in-

TABLE II. Deformation lengths ($\delta = \beta R$).

Nuclide	$B(E2)$ ($e^2 b^2$)	δ (fm) (Other work) (α, α') [a]	(p, p') [a]	(Elec.) [b]	$(^{16}O, ^{16}O')$		Present work E_{lab} (MeV)	δ^N/δ^C	δ^N (fm)
^{58}Ni	0.0728 [c]	0.94 ± 0.21	1.03 ± 0.18	0.83 ± 0.15	0.94 [d]	0.76 [e]	42	1.3 [f]	1.1
								1.2	1.0
							48	1.0	0.85
^{60}Ni	0.097 [g]	1.56 ± 0.40	1.28 ± 0.32	0.98 ± 0.15			42	1.0	0.98
							48	1.0	0.98
^{62}Ni	0.084 [g]	0.88 ± 0.17	1.70 ± 0.34	0.83 ± 0.12			42	1.0	0.90
							48	1.1	0.99
^{64}Ni	0.087 [g]	1.10 ± 0.25	1.19 ± 0.18	0.84 ± 0.17	1.3 [h]	0.87 [i]	42	1.0	0.90
							48	0.95	0.86

[a] Reference 19.
[b] (e, e') and Coulomb excitation results of Ref. 19.
[c] Reference 17.
[d] Reference 3.
[e] Reference 20.
[f] Folded potential
[g] Reference 21.
[h] Reference 22.
[i] Reference 23.

elastic scattering of ^{16}O from $^{58,60,62,64}Ni$ are tabulated in Table II. Since the Coulomb deformation length and the Coulomb deformation parameter, as determined from the quadrupole electromagnetic transition probability, depend upon the Coulomb radius used, the Coulomb radius of the target was chosen to be equal to the nuclear radius. Even though the Coulomb radius is that of a uniform charge distribution and the nuclear radius is the half radius of a diffuse distribution, for comparison purposes the Coulomb radius can be set equal to the nuclear radius since neither the elastic nor the inelastic scattering cross section is sensitive to the value of the Coulomb radius. This equality allows direct comparison between the Coulomb and nuclear deformation lengths and the deformation parameters. Since the values of deformation length sometimes differed at the two energies investigated, results for each energy are included in Table II. The $B(E2)$ values from which the Coulomb deformation length is calculated are also included. Finally, deformation lengths which represent an average of individual values deduced from inelastic scattering of α particles and protons and from electromagnetic excitations (inelastic electron scattering and Coulomb excitation) are included for comparison. The electromagnetic results also are Coulomb radius dependent, and unless the average radius used in the extraction happens to be equal to the radius used in this work, these deformation lengths will be different even if the same transition probability value is used to find the deformation length. Other recent reported results for the inelastic scattering of ^{16}O from ^{58}Ni are also included. To within the probable accuracy of the results, the table indicates the nuclear deformation length is equal to the Coulomb deformation length.

The data and the conventional analysis presented herein do not reveal any significant systematic trend in the inelastic scattering from different nickel isotopes. This is likely due to a combination of insensitivity of the analysis, statistical error in the data, and contributions from other mechanisms. The data for both the elastic and inelastic scattering are available[24] for reanalyses to include additional effects.

Further investigations of inelastic scattering of heavy ions will be fruitful for a number of reasons. One important feature is that the prominent structure in the inelastic scattering cross section allows the direct determination of the nuclear deformation length relative to the Coulomb deformation length. More experimental and computational information in this area is needed to determine if there is indeed a difference in the deformation lengths. Extensive studies to include coupled-channels calculations and multistep processes may be necessary to provide an adequate description of the inelastic process. It is noted, however (see Table II), that the results of two recent coupled channel analyses[22,23] differ greatly in the values of deformation length obtained.

The authors wish to acknowledge Dr. Steve Cotanch who derived the folded Coulomb expressions, Dr. Don Robson and Dr. Fred Petrovich for numerous discussion concerning the use of folded potentials, and Dr. Kirby Kemper, Dr. Gordon Morgan, and Dr. Jerry Artz, and Mr. Don James for their assistance in the data accumulation.

*Work supported in part by the National Science Foundation Grants Nos. NSF-GU-2612, NSF-PHY-7503767-A01, and NSF-GJ-367.

† Present address: Health Physics Division, LASL, Los Alamos, New Mexico 87545.

[1]F. Videbaek, I. Chernov, P. R. Christensen, and E. E. Gross, Phys. Rev. Lett. 28, 1072 (1972).

[2]L. West and N. R. Fletcher, in Proceedings of the Symposium on Heavy-Ion Transfer Reactions, Argonne, 1973 (unpublished), Vol. II, p. 581 [Argonne National Laboratory, Physics Division Informal Report No. PHY-1973B (unpublished)].

[3]P. R. Christensen, I. Chernov, E. E. Gross, R. Stokstad, and F. Videbaek, Nucl. Phys. A207, 433 (1973).

[4]J. L. C. Ford, Jr., K. S. Toth, D. C. Hensley, R. M. Gaedke, P. J. Riley, and S. T. Thornton, Phys. Rev. C 8, 1912 (1973).

[5]L. West, S. Cotanch, and D. Robson in *Proceedings of the International Conference on Nuclear Physics, Munich, West Germany, 1973*, edited by J. de Boer and H. J. Mang (North-Holland, Amsterdam/American Elsevier, New York, 1973), Vol. I, p. 383.

[6]F. Videbaek, P. R. Christensen, Ole Hansen, and K. Ulbak, Nucl. Phys. A256, 301 (1976).

[7]M. E. Cobern, M. Lisbona, and M. C. Mermaz, Phys. Rev. C 13, 674 (1976).

[8]R. H. Bassel, G. R. Satchler, R. M. Drisko, and E. Rost, Phys. Rev. 128, 2693 (1962).

[9]L. West, Jr., K. W. Kemper, and N. R. Fletcher, Phys. Rev. C 11, 859 (1975).

[10]G. Igo, Phys. Rev. 115, 1665 (1959).

[11]A. W. Obst, D. L. McShan, and R. H. Davis, Phys. Rev. C 6, 1814 (1972).

[12]G. R. Satchler, Phys. Lett. 39B, 495 (1972).

[13]R. Hofstadter and H. R. Collard, in *Nuclear Radii Determined by Electron Scattering*, edited by H. Schopper (Springer, Berlin, 1967).

[14]P. D. Kunz, University of Colorado (unpublished).

[15]M. Samuel and U. Smilansky, Comp. Phys. Comm. 2, 455 (1971).

[16]A. Winther and J. de Boer, A Computer Program for Multiple Coulomb Excitation, California Institute of Technology, Technical Report, 1965 (unpublished).

[17]P. M. S. Lesser, D. Cline, and J. D. Purvis, Nucl. Phys. A151, 257 (1973).

[18]M. E. Cage, A. J. Cole, and G. J. Pyle, Nucl. Phys. A210, 418 (1973).

[19]G. Bruge, J. C. Faivre, H. Faraggi, and A. Bussiere, Nucl. Phys. A146, 597 (1970).

[20]F. D. Becchetti, P. R. Christensen, V. I. Manco, and R. J. Nickles, Nucl. Phys. A203, 1 (1973).

[21]P. H. Stelson and L. Grodzins, Nucl. Data A1, 21 (1965).

[22]M. E. Cobern, N. Lisbona, and M. C. Mermaz, Phys. Rev. C 13, 674 (1976).

[23]F. Videbaek, P. R. Christensen, Ole Hansen, and K. Ulbak, Nucl. Phys. A256, 301 (1976).

[24]See AIP document No. PAPS 2052 for 10 pages of data. Order by PAPS number and journal reference from American Institute of Physics, Physics Auxiliary Publication Service, 335 East 45 Street, New York, N. Y. 10017. The price is $1.50 for microfiche or $5.00 for photocopies. Make checks payable to the American Institute of Physics. The material also appears in *Current Physics Microfilm* on the frames immediately following this journal article.